Current-voltage characteristics of many-valley semiconductors with multivalued dependence of the current on the electric field

V. V. Mitin

Institute of Semiconductors, Academy of Sciences of the Ukrainian SSR, Kiev

(Submitted October 16, 1976)

Fiz. Tekh. Poluprovodn. 11, 1233–1241 (July 1977)

The actual current-voltage characteristics are obtained for the case when a weakly heating electric current i_x flows in a classically strong transverse magnetic field H_z so that for a uniform current distribution the characteristics should be of the S-type, caused by a steep dependence of the intervalley scattering time on the heating power. It is shown that the real characteristics of n-type Ge with $i_x \parallel [110]$ and $H_z \parallel [110]$ should as a rule be single-valued. In a narrow range of electric fields, a high positive differential conductance is observed; this is associated with the fact that a high-field domain occurs near one of the surfaces parallel to the current and magnetic field, and this domain increases with the field as a result of the rapid movement towards the opposite surface of the domain walls which separate it from a weak-current domain. This type of characteristic will occur in n-type Si with $i_x \parallel [100]$ if the intervalley scattering rate is low on the surface where the high-field domain starts to form. If the rate is not low, then a given range of currents can only be realized when there is a high negative differential conductance with a current domain which moves perpendicular to the current and the magnetic field; this should lead to oscillations at a frequency which is inversely proportional to H_z.

PACS numbers: 72.80.Cw

INTRODUCTION

It is shown in Ref. 1 that S-type current–voltage characteristics (Fig. 1) may be exhibited by many-valley semiconductors at low temperatures when the intervalley scattering time τ_α decreases rapidiy with increase in the power π_α received by an electron in a valley α from the electric field E. These characteristics occur in a classically strong transverse magnetic field H_z, when π_α is governed mainly by the Hall field $E_y \gg E_x$, and are due to the fact that over a certain range $(E_c^{(l)}, E_c^{(h)})$ of values of the applied electric field E_x there is not one (as in the usual case) but three possible uniform electron distributions over the valleys, corresponding to three values of the current density i_x and Hall field E_y.

The state with a uniform current distribution and a negative differential conductance (section AB of the S-type characteristic in Fig. 1) is unstable against small quasi-neutral perturbations, as can easily be shown by a method similar to that in Refs. 2 and 3. In this paper, we study the nonuniform distribution states and the corresponding current–voltage characteristics, which we shall call the real characteristics[2,3] in contrast to the S-type form.

SOLUTION OF THE CONTINUITY EQUATIONS IN THE STEADY STATE

If the diffusion length for intervalley scattering L is very much greater than the Debye length (as is assumed here and in Refs. 4 and 5), the electron distribution over

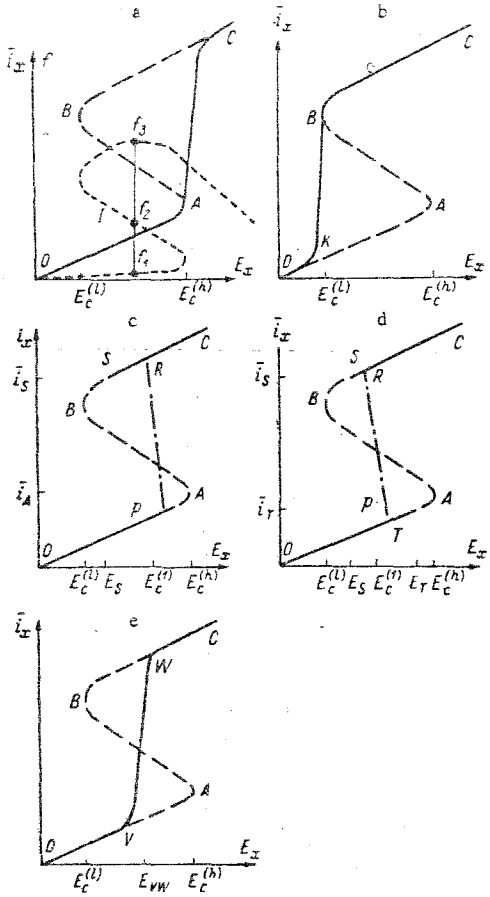

FIG. 1. Field dependences of the current $\bar{i}_x$ and the intervalley redistribution (1a) (Ref. 1). The dashed curves show the S-type current–voltage characteristics (OABC) (Ref. 1), the continuous curves depict the characteristics for a steady-state distribution, and the chain curves give the sections of the characteristics corresponding to moving current domains ($\gamma > 0$): a) $f_3 < \bar{f}_1$; b) $f_3 > \bar{f}_1$, $\mathscr{E}^+ < \mathscr{E}_c(f_3)$; c) $f_3 > \bar{f}_1$, $\mathscr{E}^+ > \mathscr{E}_c(\bar{f}_1)$; d) $f_3 > \bar{f}_1$, $\mathscr{E}_c(f_3) < \mathscr{E}^+ < \mathscr{E}_c(\bar{f}_1)$; e) $f_3 < \bar{f}_1$ for $E_x < E_{VW}$ and $f_3 > \bar{f}_1$ for $E_x > E_{VW}$.

the valleys at each point of a sample (which determines the real current–voltage characteristics) can be found from the continuity and quasineutrality equations[4,6]

$$\frac{1}{e}\operatorname{div}\mathbf{i}^{(\alpha)}=\sum_{\beta\neq\alpha}\left(\frac{n_\alpha}{\tau_\alpha}-\frac{n_\beta}{\tau_\beta}\right)+\frac{\partial n_\alpha}{\partial t},\quad \sum_{\alpha=1}^{\lambda}n_\alpha=\lambda n_0, \tag{1}$$

where n_α and $\mathbf{i}^{(\alpha)}$ are the electron density and current density in a valley α; $n_0 = n_\alpha(E_X = 0)$; λ is the number of valleys; t is time; and e is the electron charge.

Since S-type characteristics occur in weakly heating electric fields in which the diffusion coefficients $\hat{D}$ and the mobilities $\hat{\mu}$ are close to their equilibrium values calculated for $E_X = 0$ and the times τ_α change rapidly as a result of their steep dependence on the heating,[1] the only quantities which depend on E and the coordinates in Eq. (1) are τ_α and n_α (see also Refs. 5 and 6).

We shall consider a sample in which the current $i = \sum_{\alpha=1}^{\lambda} i^{(\alpha)}$ flows along the x axis, there is a classically strong magnetic field $H \parallel z$, and the dimensions 2d ($-d \le y \le d$) and 2b ($-b \le z \le b$) are small compared to the sample length 2l ($-l \le x \le l$) but are much greater than L. The distribution is therefore uniform and stable along z so that the problem is one-dimensional [$\tau_\alpha = \tau_\alpha(y)$, $n_\alpha = n_\alpha(y)$].

We shall deal first with n-type Ge, in which, for $x \parallel [110]$ and $z \parallel [1\bar{1}0]$, the valleys should be pairwise equivalent (the word valley will be used below to mean a pair of equivalent valleys) and which has S-type characteristics.[1] Taking the usual expressions for $\mathbf{i}^{(\alpha)}$ (Refs. 4 and 5), we get the following transverse field from the condition $i_y = \sum_{\alpha=1}^{\lambda} i_y^{(\alpha)} = 0$:

$$\mathcal{E}_y=-\frac{\hat{D}}{D}H\mathcal{E}_x\frac{1}{(1-af)}+\frac{a}{(1-af)}\frac{df}{dx}. \tag{2}$$

Using Eq. (2) and the fact that $\operatorname{div}\mathbf{i} = 0$ in the steady state ($\partial n_\alpha/\partial t = 0$), we can reduce Eq. (1) to the form

$$p\frac{d}{df}(pg(f)-\gamma ah(f))=\mathscr{F}(f-R), \tag{3}$$

$$g(f)=\frac{1-a^2}{1-af},\quad h(f)=\frac{1-f^2}{1-af},\quad R=\frac{\tau_1-\tau_2}{\tau_1+\tau_2},$$

$$\mathscr{F}=\frac{\tau_1+\tau_2}{\tau_1\tau_2}\tau_0,\quad \tau_0=\tau_\alpha(E_x=0), \tag{4}$$

$$p=\frac{df}{d\tau_1},\quad f=\frac{n_1-n_2}{2n_0},\quad \tau_1=\frac{y}{L},\quad L=\sqrt{D\tau_0},\quad \gamma=-\frac{\hat{D}}{D}H\mathcal{E}_xL,\quad \delta=\frac{eE}{\varkappa T}, \tag{5}$$

$$a=\frac{K-1}{K+2},\quad K=\frac{D_l}{D_t},\quad \hat{D}=\frac{\varkappa Tc}{eH^2},$$

$$D=\frac{K+2}{3}D_t,\quad D_{l,t}=C\int_0^\infty\left(\frac{m}{\tau}\right)_{l,t}\chi^{5/2}e^{-\chi}d\chi, \tag{6}$$

where $\varkappa$ is Boltzmann's constant; T is the temperature; c is the velocity of light; $\chi = \varepsilon/\varkappa T$ is the dimensionless energy; $\tau_{l,t}$ and $(1/m)_{l,t}$ are the components of the relaxation time and reciprocal effective mass tensors; l is the axis of rotation of the constant-energy ellipse, and $t \perp l$; $C = 3\varkappa Tc^2/[(K+2)e^2H^2\Gamma(5/2)]$.

S-type characteristics occur under independent energy balance conditions in the valleys,[1] when $L \gg L_\varepsilon$ [L_ε is the cooling length (Ref. 4)], so that even in weakly heating electric fields, where $|\gamma|L_\varepsilon/L \sim 1$ [see, for example, Eqs. (13) and (13') in Ref. 5], the following condition is satisfied:

$$|\gamma| \gg 1. \tag{7}$$

In order to reduce Eq. (3) to a normal differential equation, we have to know $\tau(f)$. Arguments similar to those in Ref. 5 and the analysis given below show that condition (7) means that Eq. (3) can be represented in the form of domains (and smooth domain walls), where $f(\eta)$ varies slowly and so the diffusion current components can be neglected [as well as the term pg in Eq. (3)], and abrupt domain walls, where $f(\eta)$ changes rapidly so that the currents $i_y^{(\alpha)}$ are almost constant [the term in the braces of Eq. (3) is constant)]. In the abrupt domain walls, the right side of Eq. (3) is negligible and so we can assume that, as in the uniform case, $\tau_{1,2}$ are local functions of the powers $\pi_{1,2}$ (Ref. 5), which, from inequality (7) and the condition $L \gg L_\varepsilon$, are also local, i.e.,

$$\pi_{1,2}=\frac{(\mathbf{i}^{(1,2)}\mathbf{E})}{n_{1,2}}\simeq\frac{e^2D}{\varkappa T}\left(\frac{\hat{D}}{D}HE_x\right)^2\frac{(1\mp a)}{(1-af)^2}. \tag{8}$$

Since the domain walls are so narrow, we can also neglect the diffusion components in calculating the current i_x, and so

$$i_x \simeq -\frac{e^2\bar{D}}{\varkappa T}\lambda n_0 H E_y \simeq e\lambda n_0 e\frac{\bar{D}}{D}E_x\frac{1}{(1-af)} \tag{9}$$

will depend on y only via f(y).

As in Refs. 2, 5, 7, and 8, we shall study the solutions of Eq. (3) in the phase plane pf. The singular points can be found by putting the right side of Eq. (3) equal to zero for p = 0; this then corresponds to the equation in the uniform case, f = R, and in the interval of fields $(E_c^{(l)}, E_c^{(h)})$, this has three solutions (Ref. 1), $f = f_{1,2,3}$ (Fig. 1a). When $E_c^{(l)} < E_x < E_c^{(h)}$, f_1 and f_3 are saddle points and f_2 is a focus or node. As a result of condition (7), the phase plane has both abrupt (high value of the derivative dp/df) and smooth (dp/df is small) separatrices, and one kind can transform to the other. The equations for the first kind

$$p=\frac{\gamma a}{g(f)}[h(f)-h(f_i)],\quad (f_i=f_1,\ f_3) \tag{10}$$

are similar to those for abrupt domain walls.[5] Putting $h(\bar{f}_i) = h(f_i)$ in Eq. (10), we find the point $\bar{f}_i$ at which the separatrix which comes from f_i should intersect the f axis,

$$f_{cr}=\frac{a-f_i}{1-af_i}. \tag{11}$$

When $f_i < f_{cr}$, we have $\bar{f}_i > f_i$, and when $f_i > f_{cr}$, then $\bar{f}_i < f_i$, i.e., f_i and $\bar{f}_i$ on the f axis lie on opposite sides of f_{cr} and they coincide when $f_i = f_{cr}$. Here

$$f_{cr}=\frac{1}{a}(1-\sqrt{1-a^2}), \tag{12}$$

which belongs to the region (−1, 1), is the solution of the equation dh(f)/df = 0.

The lines of zeros (dp/df = 0) are defined by the equations

$$p_{1,2}=\frac{1}{2}\gamma a\frac{dh/df}{dg/df}\pm\sqrt{\left(\frac{1}{2}\gamma a\frac{dh/df}{dg/df}\right)^2+\mathscr{L}\frac{f-R}{dg/df}}. \tag{13}$$

For $\gamma > 0$, the smooth separatrices are close to $p_2(f)$ for $f < f_{cr}$ and to $p_1(f)$ for $f > f_{cr}$. At distances of the order of $1/|\gamma|$ from f_{cr}, the behavior of $p_{1,2}$ and of the smooth separatrices depends on the sign of $(f-R)_{f=f_{cr}}$, which is determined by the relationship between f_{cr} and f_1, f_2, and f_3 ($f - R < 0$ if $f < f_1$ or $f_2 < f < f_3$, and $f - R > 0$ if $f_1 < f < f_2$ or $f > f_3$). Equations (10) and (13) define two characteristic lengths: The extended length $L_2 = L|\gamma|/\mathscr{L} \gg L$ and the reduced length $L_1 = L/|\gamma| = \left(\frac{\bar{D}}{D}H\mathscr{E}_x\right)^{-1} \ll L$ and this completely justifies Eqs. (8) and (9) and the idea about domains and abrupt domain walls. In what follows we assume that the samples are thick compared to the extended length ($2d \gg L_2$).

In order to choose the phase trajectories, we have to take into account the boundary conditions[2,5] which are imposed on the currents $i_y^{(\alpha)}$ on the surfaces $y = \pm d$ (Refs. 4 and 5) and which in the notation of Eqs. (4)–(6) have the form

$$(pg(f)-\gamma ah(f))|_{y=\pm d}=\mathscr{L}^{\pm}(f^{\pm}-R^{\pm}), \tag{14}$$

where $f^{\pm} = f(y = \pm d)$, and $\mathscr{L}^{\pm}$ and $R^{\pm}$ are obtained from $\mathscr{L}$ and R when $1/\tau_{1,2}$ are replaced by $S_{1,2}/L$ ($S_{1,2}^{\pm}$ are the intervalley scattering rates in valleys 1 and 2 on the surfaces $y = \pm d$). The rates $S_{1,2}^{\pm}$ are parameters which in general depend on the electric field. We shall consider the surface scattering mechanisms for which $S_{1,2}^{\pm}$ depend less strongly than $\tau_{1,2}$ on $\bar{\tau}_{1,2}$ (Ref. 5) so that we can take $S_1^{\pm} \simeq S_2^{\pm} \simeq S^{\pm}$ and $R^{\pm} \simeq 0$.

The relationships between f_{cr} and f_1, f_2, and f_3 define both the behavior of $p_{1,2}(f)$ near f_{cr} and also the positions of the points $\bar{f}_{1,3}$; they thus affect the shape of the phase trajectories. We shall first study the case $f_3 < f_{cr}$. Figure 2a shows the phase trajectories of Eq. (3) and the boundary conditions (14) for $\gamma > 0$. It is clear that for all positive rates $S^{\pm}$, the only possible trajectories are those which pass close to the singular point f_1; if $\mathscr{L}^+ > \mathscr{L}_c^+(f_1)$, then we get the phase trajectory ABC, and if $\mathscr{L}^+ > \mathscr{L}_c(f_1)$, we have DEF. Here

$$\mathscr{L}_c(f)=\frac{|\gamma|ah(f)}{|f|}=|\gamma|a\frac{1-f^2}{|f|(1-af)}. \tag{15}$$

Thus, in the whole of the region $(E_c^{(l)}, E_c^{(h)})$, only quasiuniform distributions with $f = f_1$ (f_1-domain) and $i_x = i_x(f_1)$ are possible. When $E_x > E_c^{(h)}$, there is a transition over a narrow range of fields from an f_1-domain to an f_3-domain. This last type of domain originates at the surface $y = +d$; as the field increases, the smooth domain wall which separates this domain from the f_1 domain moves towards the surface $y = -d$. The actual current–voltage characteristics for this case are shown in Fig. 1a.

In a similar way, we can find the phase trajectories and characteristics corresponding to other relationships between f_2, f_3, and f_{cr}. If

$$f_3 < f_1 = \frac{a-f_1}{1-af_1} \tag{16}$$

(we always have $f_1 \ll 1$), then changes occur in the phase plane but they do not affect the choice of the trajectories, which pass as before close to f_1 and the actual characteristics are defined by the curve OAC (Fig. 1a). If the opposite inequality to (16) is satisfied, then of course $f_3 > f_{cr}$, and it is clear from Fig. 2b that there are several phase trajectories which satisfy the same boundary conditions. As before, only the rate S^+ affects the choice of trajectories. For small rates S^+, when

$$\mathscr{L} < \mathscr{L}_c(f_3), \tag{17}$$

the trajectories in the interval $(E_c^{(l)}, E_c^{(h)})$ (see ABC in Fig. 2b) can only pass near f_3 (f_3 domain) and $i_x = i_x(f_3)$. When $E_x < E_c^{(l)}$, an f_1 domain appears near the surface $y = -d$, and over a narrow range of fields $[E_c^{(l)} - E_x \ll E_c^{(l)}]$ as the field E_x decreases, the domain wall which separates the f_1 from the f_3 domain moves towards $y = +d$, so that the current–voltage characteristics are defined by the curve OKBC in Fig. 1b. If S^+ is not small [$\mathscr{L}^+ > \mathscr{L}_c(f_3)$ Eq. (17)], then for

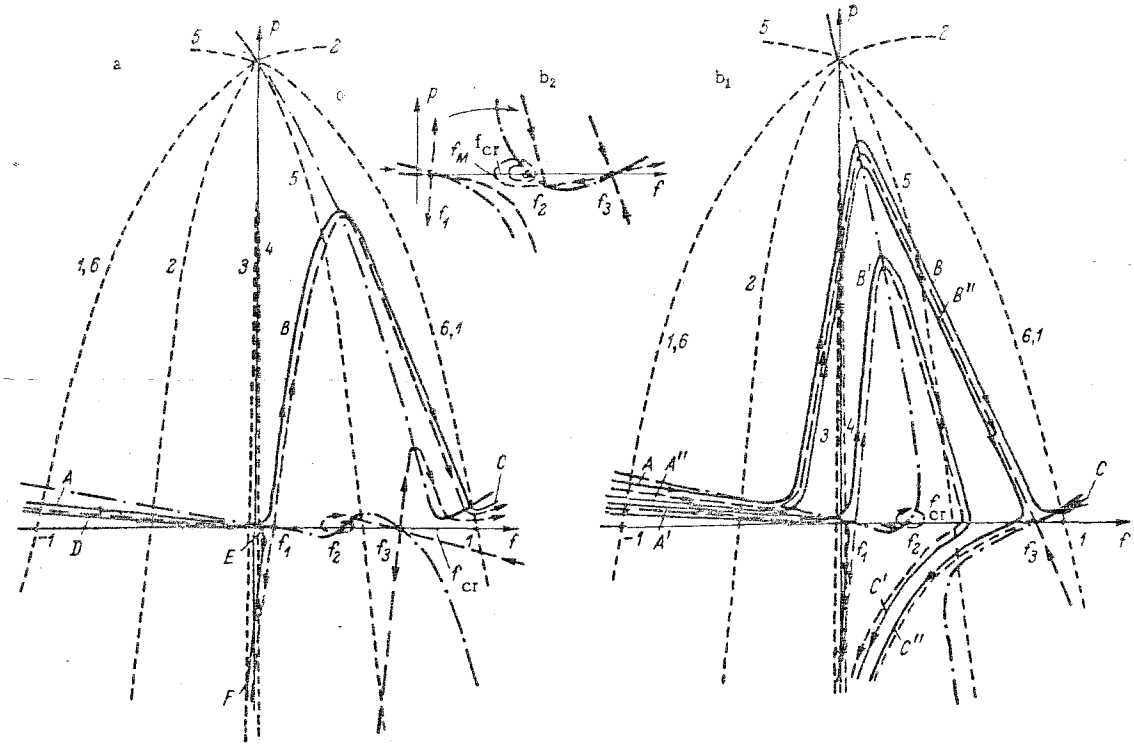

FIG. 2. Phase trajectories of Eq. (3) (continuous lines) for $\gamma > 0$. The dashed curves are the separatrices, the chain curves the lines of zeros, and the dotted curves the boundary conditions on the surfaces $y = -d$ (1-3) and $y = +d$ (4-6). 1) $\mathcal{L}^- = 0$; 2) $\mathcal{L}^- \approx \gamma$; 3) $\mathcal{L}^- \gg \gamma$; 4) $\mathcal{L}^+ \gg \gamma$; 5) $\mathcal{L}^+ \approx \gamma$; 6) $\mathcal{L}^+ = 0$. a) $f_3 < f_{cr}$; b) $f_3 > \bar{f}_1$; b_1) $f_2 < f_{cr}$; b_2) $f_{cr} < f_2 < f_1$.

$$\mathcal{L}_c(f_M) > \mathcal{L}^+ > \mathcal{L}_c(f = \max[f_1, f_2]) \qquad (18)$$

the phase trajectories can pass close to both f_1 (A'B'C') and to f_3 (A"B"C"), but there are no trajectories which pass simultaneously close to both saddle points, i.e., there are no two-domain solutions. In Eq. (18), f_M is the point where the smooth separatrix from the saddle point f_3 ($f_1 \leq f_M \leq f_2$) cuts the f axis. This point only exists when $f_2 > f_{cr}$ and part of the phase plane for this case is shown in Fig. 2b$_2$; when $f_2 < f_{cr}$ in Eq. (18), then $\mathcal{L}_c(f_M) \to \infty$. If E_X decreases [$E_X < E_C^{(h)}$], then f_M increases and $\mathcal{L}_c(f_M)$ falls, so that condition (18) is no longer satisfied [as $E_X \to E_C^{(l)}$, we have that $f_2 \to f_3$ and also that $f_M \to f_3$, and so $\mathcal{L}_c(f_M) \to \mathcal{L}_c(f = \max[f_1, f_2]) \to \mathcal{L}_c(f_3)$, and the solution f_3 suddenly disappears in a field E_S, which can be found from the condition $\mathcal{L}_c(f_M) = \mathcal{L}^+$). If $\mathcal{L}^+ > \mathcal{L}_c(f_1)$, the solution $f = f_1$ is possible over the whole of the range $(E_c^{(l)}, E_c^{(h)})$ and disappears suddenly when $E_c > E_c^{(h)}$. If $\mathcal{L}^+ < \mathcal{L}_c(f_1)$, the solution $f = f_1$ occurs in the interval $(E_c^{(l)}, E_T)$ and the field E_T is defined by the condition $\mathcal{L}_c(f_2) = \mathcal{L}^+$. The real current–voltage characteristics for $\mathcal{L}^+ > \mathcal{L}_c(f_1)$ and $\mathcal{L}^+ < \mathcal{L}_c(f_1)$ are shown in Figs. 1c and 1d. In contrast to the cases considered above (Figs. 1a and 1b), there is no transition here as the field E_X changes from phase trajectories passing near one saddle point to trajectories passing near the other and a typical feature is the presence of jumps in the current[1] [at fields of E_S and $E_C^{(h)}$ (Fig. 1c) and E_S and E_T (Fig. 1e)] and the current ranges (i_A, i_S) in Fig. 1c and (i_T, i_S) in Fig. 1e cannot be realized for a steady-state distribution.

We have analyzed the current–voltage characteristics under conditions where the sign of the inequalities (16) and (17) is retained over the whole of the interval $(E_C^{(l)}, E_C^{(h)})$. We shall now consider cases where the sign of inequality (16) changes, and we shall put $S^+ = 0$. Figure 1a shows a typical $f(E_X)$ dependence obtained from Ref. 1. As E_X increases, f_1 rises and f_3 reaches a maximum and then decreases. Inequality (16) can therefore be satisfied when $E_X < E_{VW}$ and for $E_X > E_{VW}$, the opposite inequality can hold. The field E_{VW} corresponds to the special case $f_3 = \bar{f}_1$. The actual characteristics are defined by the curve OVWC (Fig. 1e) and the section VW arises from the fact that as the field increases, the abrupt domain wall which separates the f_1-domain from the f_3 domain shifts towards the surface $y = -d$ and the f_3 domain increases.[2)]

A change in the sign of inequality (17) with increasing E_X does not produce fundamentally new characteristics.

We have considered the phase trajectories for $\gamma > 0$; for $\gamma < 0$, we have to replace p by $-p$ and y by $-y$ and reverse the directions of all the trajectories in Fig. 2. For symmetric boundary conditions, this can lead to a change in the conductance if $f_3 > \bar{f}_1$. In particular, if $\mathcal{L}^+ < \mathcal{L}_c(f_3)$, and $\mathcal{L}^- > \mathcal{L}_c(f_3)$, the characteristics are given by Fig. 1b or 1e when $\gamma > 0$ and by Fig. 1c or 1d when $\gamma < 0$. Since $\gamma \sim H\mathcal{E}_X$ from Eq. (5), rectifying characteristics occur and there is an odd magnetoresistance.

STEADY-STATE DOMAIN MOTION

For a steady-state distribution, we cannot get currents in the ranges (i_A, i_S) and (i_T, i_S) (Figs. 1c and 1d) and so we shall look for the solution of Eq. (1) for this case in the class of standing waves,[2,7,8] i.e., we shall assume that the solution is a nonuniform distribution $f(\eta)$ which is moving at a constant velocity $u = u_0 \gamma a L/\tau_0$. Equation (1) then takes the form of Eq. (3) except that h is replaced by $h - u_0 f$ and η by $\eta - \gamma a u_0 t/\tau_0$. As $t \to -\infty$, the solution for thick samples will approach some closed

integral curve (limit cycle) under a wide variety of boundary conditions.[2,7,8] For $|\gamma| \gg 1$, limit cycles will exist if f_2 is the center and this determines the domain velocity

$$u_0 = \frac{dh}{df}\Big|_{f=f_2} = \frac{a - 2f_2 + af_2^2}{(1 - af_2)^2}. \quad (19)$$

For thick samples ($d \gg L_2$), the main contribution to the integral

$$\int_{-d}^{+d} i_x\, dy = 2di_x$$

comes from the regions near the rest points and therefore a given current $\bar{i}_x$ in the range $(i_x(f_1), i_x(f_3))$ can only be achieved if the separatrices coming from f_1 and f_3 either coincide or are close to each other. It is easily shown that the separatrices coincide and the limit cycle passes near f_1 and f_3 if

$$f_3 + f_1(1 - af_3) - 2f_2 + af_2^2 = 0. \quad (20)$$

When $E_x = E_c^{(l)}$, we have $f_2 = f_3$, and the right side of Eq. (20) is negative; when $E_x = E_c^{(h)}$, then $f_2 = f_1$ and it is positive. Equation (20) therefore always has a solution and this determines the field $E_c^{(1)}$ and the velocity $u_0 = u_0(f_2[E_c^{(1)}])$. In the neighborhood of the field $E_c^{(1)}$, the current $\bar{i}_x$ changes due to variations in the size of the f_1 and f_3 domains [as $E_x - E_c^{(1)}$ ($E_c^{(1)} - E_x$) increases, the f_3 (f_1) domain decreases]. The motion of the f_3 (f_1) domain for $E_x > E_c^{(1)}$ ($E_x < E_c^{(1)}$) corresponds to the motion of the i_x current domain and the domain of the Hall field E_y [see Eqs. (2) and (9)][3]. We are considering a solution with only one moving domain because it is shown in Refs. 10 and 11 and in a number of other papers (and this proof can be repeated here) that for equations like Eq. (3), the solutions with a large number of moving domains are unstable.

Figures 1c and 1d show the sections PR corresponding to the solution with a moving domain.[4] If the size along y is infinite, the section PR will be steady-state and the real characteristics will have the same form as in the case of the S-type overheating.[2,3,8] In thick but finite samples, which require special treatment, the steady-state conditions are violated when the domain emerges at the surface. If the rates $S^{\pm}$ on the surface are high ($\mathscr{L}^{\pm} \gg |\gamma|$), they affect the velocity of the domains, which easily recombine and reform on the surfaces. At a fixed point, therefore, domains will pass at a frequency which is determined by the time a domain takes to travel from one surface to the other,

$$\omega_1 = 2\pi \frac{|u|}{2d} = \pi \frac{cE_c^{(1)}}{|H|d} a\,|u_0|. \quad (21)$$

If $\mathscr{L}^{\pm} \gg |\gamma|$, then on arrival at the surface, a domain will recombine (and also reform at the opposite surface) in a time $\sim\tau = \tau_1\tau_2/(\tau_1 + \tau_2)$, thus reducing the characteristic frequency ω. In the thick samples that we are considering ($d \gg L_2$), $\omega \sim \omega_1$ since $\omega_1 \ll \omega_2$ (here $\omega_2 = 2\pi/\tau$). It is clear that in bounded samples, the current will oscillate at a frequency $\sim\omega$; the theory of these oscillations requires separate treatment.

We shall now consider the current–voltage characteristics of n-type Si. If $x \parallel [100]$ in n-type Si, then the valleys 1 and 1' in the yz plane have the same mobility along y, whatever the orientations of y and z relative to the crystallographic axes. They will therefore be equally heated ($\pi_1 = \pi_{1'}$) and occupied ($n_1 = n_{1'}$); if we put $f = 2(n_1 - n_0)/n_0 \equiv -(n_2 - n_0)/n_0$, then Eq. (1) can again be reduced to Eq. (3), but with new q, h, $\mathscr{L}$, and R. An analysis of the new equation shows that over the whole of the range $(E_c^{(l)}, E_c^{(h)})$ the opposite inequality to (16) holds $[-f_2 > \bar{f}_1, E_T < E_c^{(h)}]$, and so the real characteristics are determined for small (Fig. 1b) and large (Fig. 1d) rates $S^{\pm}$. In the latter case, oscillations caused by the movement of domains should occur for a given current in the range (i_T, i_S).

In Ref. 12, current oscillations at a frequency of ~ 1 MHz were observed for S-type characteristics in n-type Si. This frequency agrees in order of magnitude with ω_1 from Eq. (21) if we put $u_0 \approx 1$ and we have (see Ref. 12) $E_c^{(l)} = 100$ V/cm, H = 20 kOe, and 2d = 0.6 mm. It is not possible to make a more detailed comparison between theory and experiment since no other experimental results apart from those in the short communication of Ref. 12 are known to us.

Thus, for the S-type characteristics considered here, the continuity equation (3), which defines the dependences of the electron densities in each of the valleys on the coordinates and hence the real current–voltage characteristics, differs from the normal equation, which is solved for S-type overheating characteristics[2,3,8] by the presence of an additional term $(-p\gamma a\,dh/df)$, which makes it easy to compare Eq. (3) with the continuity equation for N-type characteristics[2,8] (see also Ref. 10). For the real characteristics shown in Figs. 1a, 1b, and 1e, the high-field domain therefore increases with the field as a result of a rapid domain wall displacement similar to that for steady-state field domains in Ref. 2. There is a similar analogy between the movement of current domains here (Figs. 1c and 1d) and of field domains in Refs. 2, 7, and 8.

The actual current–voltage characteristics depend not only on the surface conditions (compare Figs. 1b, 1c, and 1d) but also on the semiconductor band structure. Thus, in n-type Si ($\mathbf{i} \parallel [100]$) it is only possible to get the characteristics depicted in Figs. 1b and 1d, while in n-type Ge ($\mathbf{i} \parallel [100]$, $\mathbf{H} \parallel [1\bar{1}0]$), where f_1 is close to unity, the characteristics must be those shown in Figs. 1a and 1e, although at very low temperatures the case $f_3 (E_c^{(l)}) > \bar{f}_1$ is not in principle excluded and characteristics like Figs. 1b and 1d are possible.

The author is sincerely grateful to Z. S. Gribnikov for the trouble he took in getting acquainted with the manuscript of the present paper and for valuable comments, to V. A. Kochelap for useful discussions, and to O. G. Sarbei for a discussion of the results and for drawing the author's attention to certain features of the current–voltage characteristics in Ref. 12.

[1)]Jumps in the current in a magnetic field were predicted earlier in Ref. 9 for S-type overheating characteristics.

[2)]Although, as a rule, the principal decrease in f_3 takes place (Fig. 1a) for $E_x > E_c^{(h)}$, two other situations can, in principle, occur: a) $f_3 \geqslant \bar{f}_1$ for $E_x \leqslant E_{LM}$; b) $f_3 < \bar{f}_1$ for $E_x < E_{VW}$ and $E_x > E_{LM}$, $f_3 > \bar{f}_1$ for $E_{VW} < E_x < E_{LM}$.

The characteristics in case b) for the range $E_x < E_{LM}$ are described by curve OEBC in Fig. 1b (OVWC in Fig. 1d) and for $E_x \sim E_{LM}$ in a narrow range of fields, the current falls from a value $i_x[f \simeq f_2(E_{LM})]$ to $i_x[f \simeq f_1(E_{LM})]$ (N-type negative differential conductance); in the region $E_x > E_{LM}$, the characteristics are described by the curve OAC (Fig. 1a). A test of the stability by the usual methods[2,3] shows that this N-type negative differential conductance section is stable (for a given voltage) since it is caused by the movement towards the surface y = + d of an abrupt domain wall so that the F_1 domain increases and the current falls.

[3)] See Ref. 10 for the motion of current domains (filaments) in a magnetic field under short-circuit conditions in the y direction ($E_y = 0$) and S-type overheating characteristics.

[4)] We shall make two comments about the PR sections. First, they can also be drawn on Figs. 1a, 1b, and 1d because Eq. (3) has, in addition to the steady-state solution which satisfies the boundary conditions (14), a standing-wave solution. The boundary conditions, which are logically taken at $u_0 = 0$, allow the moving domain to be stabilized at the surface and so the current–voltage characteristics shown in Figs. 1a, 1b, and 1d should be realized (see also Ref. 2 for the case of N-type characteristics), although the final answer can only be obtained after the temporal equation has been solved for a bounded sample with allowance for Eq. (14). Second, it is possible to get cases when the field E_T (E_S) is smaller (greater) than E_c[1]. Then, in a narrow range of currents i_x greater (smaller) than i_T (i_S), there are no standing-wave solutions and we have to look for more complex solutions which depend on t.

[1]V. V. Mitin, Phys. Status Solidi B 48, 125 (1972).
[2]V. L. Bonch-Bruevich, I. P. Zvyagin, and A. G. Mironov, Domain Electrical Instability in Semiconductors, Consultants Bureau, New York (1975).
[3]F. G. Bass, V. S. Bochkov, and Yu. G. Gurevich, Fiz. Tekh. Poluprovodn. 7, 3 (1973) [Sov. Phys. Semicond. 7, 1 (1973)].
[4]É. I. Rashba, Z. S. Gribnikov, and V. Ya. Kravchenko, Usp. Fiz. Nauk 119 3 (1976).
[5]Z. S. Gribnikov and V. V. Mitin, Phys. Status Solidi B 68, 153 (1975).
[6]Z. S. Gribnikov, V. A. Kochelap, and V. V. Mitin, Zh. Eksp. Teor. Fiz. 59, 1828 (1970) [Sov. Phys. JETP 32, 991 (1971)].
[7]M. E. Levinshtein, Yu. K. Pozhela, and M. S. Shur, The Gunn Effect [in Russian], Sovetskoe Radio, Moscow (1975).
[8]A. F. Volkov and Sh. M. Kogan, Usp. Fiz. Nauk 96, 633 (1968) [Sov. Phys Usp. 11, 881 (1969)].
[9]V. S. Bochkov, A. I. Vakser, and Yu. G. Gurevich, Fiz. Tekh. Poluprovodn 8, 2024 (1974) [Sov. Phys. Semicond. 8, 1317 (1974)].
[10]A. K. Zvezdin and V. V. Osipov, Zh. Eksp. Teor. Fiz. 58, 160 (1970) [Sov. Phys. JETP 3, 90 (1970)].
[11]A. A. Bulgakov, E. A. Kaner, S. I. Khankina, and V. M. Yakovenko, Zh. Eksp. Teor. Fiz. 64, 331 (1973) [Sov. Phys. JETP 37, 171 (1975)].
[12]L. F. Kurtenok, S. M. Ryabchenko, and O. G. Sarbei, Pis'ma Zh. Eksp. Teor. Fiz. 20, 319 (1974) [JETP Lett. 20, 142 (1974)].

Translated by R. F. Kelleher